NASA Technical Memorandum 78986

CORRELATION OF COMBUSTOR ACOUSTIC POWER LEVELS INFERRED FROM INTERNAL FLUCTUATING PRESSURE MEASUREMENTS

U. H. von Glahn
Lewis Research Center
Cleveland, Ohio

TECHNICAL PAPER to be presented at the
Ninety-sixth Meeting of the Acoustical Society of America
Honolulu, Hawaii, November 26-December 1, 1978

NASA Technical Memorandum 78986

CORRELATION OF COMBUSTOR ACOUSTIC POWER LEVELS INFERRED FROM INTERNAL FLUCTUATING PRESSURE MEASUREMENTS

U. H. von Glahn
Lewis Research Center
Cleveland, Ohio

TECHNICAL PAPER to be presented at the
Ninety-sixth Meeting of the Acoustical Society of America
Honolulu, Hawaii, November 26-December 1, 1978

CORRELATION OF COMBUSTOR ACOUSTIC POWER LEVELS INFERRED FROM INTERNAL FLUCTUATING PRESSURE MEASUREMENTS

by U. H. von Glahn

National Aeronautics and Space Administration
Lewis Research Center
Cleveland, Ohio 44135

ABSTRACT

Combustion chamber acoustic power levels inferred from internal fluctuating pressure measurements are correlated with operating conditions and chamber geometries over a wide range. The variables include considerations of chamber design (can, annular, and reverse-flow annular) and size, number of fuel nozzles, burner staging and fuel split, airflow and heat release rates, and chamber inlet pressure and temperature levels. The correlated data include those obtained with combustion component development rigs as well as engines.

INTRODUCTION

In recent years, significant progress has been made in reducing the fan and jet exhaust noise generated by aircraft gas turbine engines. As these major noise sources were reduced, other noise sources were uncovered and constitute new acoustic thresholds or floors. One of the more significant of these noise sources is combustor-associated noise. This noise originates as part of the combustion process during which a large amount of chemical energy in the form of heat is released.

Combustion noise is associated with low frequencies, usually less than 4000 Hz. Consequently, combustion noise in the far-field is often difficult to distinguish from jet noise, particularly at approach conditions where the former most frequently dominates the low frequency portion of

the overall engine noise spectrum. For takeoff conditions, jet noise usually equals or dominates combustion noise. In both cases, combustion noise propagated to the far-field is attenuated by the turbine and, to a lesser extent, by the exhaust nozzle. However, in the case of afterburners or duct burners, such as proposed for some variable-cycle inverted-velocity profile engine concepts (ref. 1), there is no turbine to attenuate the combustion noise. Consequently, for such applications, combustion noise may be significant for both takeoff and landing.

In the present study, combustion chamber acoustic power levels inferred from internal measurements of fluctuating pressure signals are correlated with operating conditions and chamber geometries over a wide range. The variables include considerations of chamber size, number of flame sites (number of fuel nozzles), combustion staging, airflow and combustion heat release rates, chamber pressure level, and chamber inlet temperature. The data base for the present correlation effort was obtained from the results published in references 2 to 8.

BACKGROUND

Data Bank

Extensive measurements of internal fluctuating pressures have been obtained for a variety of combustor types and sizes. These measurements include data taken in component development rigs (refs. 2 to 6), as well as data taken with engines (refs. 7 and 8). The objective of these programs was, in part, to determine the variation of combustor noise with chamber design and operating parameters. In the full-scale component development rig programs, fluctuating pressure measurements were obtained with both can-type and complete annular-type combustors. In addition, 90° sectors of annular combustors were also tested. The engine tests included a can-type combustor (ref. 7) and a reverse-flow annular combustor (ref. 8).

Details of the combustors, instrumentation, test procedures, and range of operating parameters are given in the references cited previously. Sketches of a number of representative combustors are shown in figure 1. It should be noted that much of the combustor development rig data

was "piggy-backed" as part of Phases I and II of the NASA Experimental Clean Combustor Program in which internal fluctuating-pressure data were obtained during combustion-product emission tests.

The overall power level (OAPWL) values used herein were calculated from measured fluctuating pressures obtained either within the combustion chamber or near the chamber exit plane. In calculating the overall power levels in the references and herein, the fluctuating pressures were assumed to be acoustic and were corrected for frequency response (where applicable). The sound power level (re 10^{-13} watts) at each measurement plane was calculated assuming plane wave propagation of the fluctuating pressure disturbance. The effect of impedance changes, flow velocity, and area were incorporated into the power level calculation where applicable.

Published Combustor Noise Correlations

In references 6 and 9 several combustion noise correlations are presented. Values of OAPWL as a function of the recommended correlating parameters are shown in figure 2 for several selected combustion chamber types and over various ranges of operating conditions. The correlating parameters given in references 6 and 9 apply to the fluctuating pressure measurements obtained in component development rigs and/or engines, depending on the particular reference, as indicated in the figure.

The Pratt and Whitney Aircraft combustion noise correlation of OAPWL (ref. 6) is given by the following relationship expressed in the nomenclature used herein:

$$\mathrm{OAPWL} \propto 10 \log \left| \frac{1}{N_F} A^2 P_3^2 \left(\frac{W\sqrt{T_3}}{P_3 A} \right)^4 \left(1 + \frac{H_f F_{ST}}{C_p T_3} \right)^2 F_b^2 \right| \qquad (1)$$

The General Electric combustion noise correlation of OAPWL for combustor development rig data (ref. 9) is given by the following relationship, again expressed in the nomenclature used herein:

$$\text{OAPWL} \propto 10 \log \left[\frac{W^{3.5}}{A^{2.5}} \left(\frac{T_3}{P_3} \right)^2 \Delta T \right] \tag{2}$$

The General Electric combustion noise OAPWL correlation parameters for engine data (ref. 9) is given by the following relationship, also expressed in the nomenclature used herein:

$$\text{OAPWL} \propto 10 \log \left[W(\Delta T)^2 \left(\frac{P_3}{T_3} \right)^2 \right] \tag{3}$$

The selected data shown in figure 2 represent the acoustic power level of an individual burner (combustor); that is, in the case of an engine using can-type combustors, the acoustic power levels shown are those for a single combustor can. In the case of the 90° sector combustors, the data were adjusted to a full annular combustor by making the necessary air flow, area and fuel nozzle number adjustments to the appropriate parameters and adding 6 dB to the calculated acoustic power levels. The following is a brief discussion of the data and its trends shown in figure 2.

It is apparent that significant differences, as well as scatter, exist in the acoustic power levels for the various combustors represented by the data in figure 2 using the correlation parameters shown. In the region of low air flow rates and pressures (JT8D-17 and J-52 can-type combustors), the inclusion of the number of fuel nozzles, suggested in reference 6, over-predicts the effect of this variable on the OAPWL while the omission of this variable (ref. 9) underpredicts the effect of this factor. The data correlations shown in figure 2 suggest also that the scope of a correlation curve faired through the data would vary with combustion air flow rate and pressure level. Finally, of the two correlations given in reference 9, the combustor development rig correlation parameters appear to give a somewhat better correlation for both rig and engine data than those recommended for correlating engine data.

PRESENT COMBUSTION NOISE CORRELATION CONCEPT

General

The correlation method for OAPWL advanced herein is predicated on the concept that combustion noise is directly related to and a prime function of the combustion heat release rate, Q, associated with the combustion process. The ratio of OAPWL to Q yields a thermoacoustic efficiency for the combustion process. A representative plot of OAPWL as a function of the heat release rate, Q, is shown in figure 3. The solid curves shown in the figure represent various thermoacoustic efficiencies. The crosshatched region shown in the figure represents the data bank of the available combustion noise data (refs. 2 to 8). Also shown for comparison in the figure, by the dashed line, are acoustic data obtained from rocket engines (ref. 10). The thermoacoustic efficiencies for aircraft engine-type combustors vary from about 0.0001 to 0.005 percent. Note that, in contrast, rocket engine thermoacoustic efficiencies are of the order of 0.5 percent or at least two orders of magnitude greater than aircraft engine-type combustors.

Variation of Power Level With Combustion Heat Release Rate

A detailed plot of OAPWL as a function of the combustion heat release rate is shown in figure 4 for the combustors previously discussed in figure 2 (JT8D-109 and YF-102 engines; and the D-13, II-11, JT8D-17, J-52, and Vorbix S-23 combustors tested in combustor development rigs). The data shown in figure 4 thus include can-type, annular (complete and 90° segment), and annular with reverse flow combustors. Also shown in the figure are curves of constant thermoacoustic efficiency.

Considering first the rig and engine data at high heat release rates, it is apparent that the thermoacoustic efficiency for a particular combustor is substantially constant. A deviation from this trend occurs for both sets of engine data when the combustion pressure levels approaches the operating design pressure ratios for the combustors. As the design pressure ratios are approached, the thermoacoustic efficiencies become

somewhat lower. This trend is not observed with the data obtained in combustion development rigs because the test combustion pressure levels were significantly below the design pressure ratio.

Effect of low heating rates and low pressure. - Although the thermoacoustic efficiencies are substantially constant for a given combustor at high combustion heat release rates, they vary considerably at low combustion heat release rates (J-52 and JT8D-17 data). With low combustion heat release rates, the thermoacoustic efficiency increases significantly, as shown in figure 4, primarily with increases in air flow rate and secondarily with a small increase in the combustion pressure.

Effect of fuel nozzle number. - A comparison of the JT8D-17 (one fuel nozzle) and J-52 (four fuel nozzles) data shows that an increase in the number of fuel nozzles in the same combustor configuration decreases the OAPWL at a constant combustion heat release rate, Q.

CORRELATION OF COMBUSTOR NOISE DATA

As stated previously, herein the prime variable in correlating the OAPWL associated with the combustion process is the combustion heat release rate, Q. In order to obtain a general correlation, however, additional parameters had to be considered. These considerations included: (1) normalization of the heat release rate for secondary considerations of air flow rate and chamber pressure and temperature conditions, and (2) normalization of the data to account for chamber geometry, including size, number of fuel nozzles, burner staging and fuel split for those combustors having burner staging. The following sections will consider first the flow-thermal effects and then the chamber geometry.

Effects of Secondary Flow and Thermal Parameters

Flow parameter. - It was determined that inclusion of the flow parameter given in reference 6 as $W\sqrt{T_3}/P_3A$, (in the present nomenclature) and which herein is rewritten as the chamber inlet Mach number, M_3, was a necessary parameter in the correlation of combustion noise. However, it was necessary also to eliminate the effect of the P_3-term which

was accomplished by multiplying the flow parameter by the ratio P_3/P_0. Additionally, a temperature ratio, $T_3/T_{AV} = 2T_3/(T_4 + T_3)$, was included to provide the best correlation of the data.

Combustor design pressure ratio. - As indicated earlier in the discussion of figure 4, the OAPWL decreases as the combustor design pressure ratio is approached. In order to correlate these data with those at low and intermediate pressure ratios for the same combustor, an empirical term was included to account for this reduction. This term is given by $\left[1 + (P_3/P_D)^3\right]$.

Summation of preceding correlation parameters. - The incorporation of the preceding flow and thermal correlation parameters with the OAPWL and Q terms is given by the following relationship:

$$\text{OAPWL} + 10 \log \left[1 + (P_3/P_D)^3\right] \propto 10 \log \left[Q M_3 (P_3/P_0)(T_3/T_{AV})\right] \qquad (4)$$

The previously selected combustor noise data shown in figure 4 are now shown in figure 5 in the parameters given by equation (4). It is apparent that generally good correlation is achieved for each individual combustor. However, the data for each combustor still fall on separate curves.

Examination of the parameters in the abscissa in figure 5 indicates that they can be rearranged to constitute a recognizable acoustic term with several modifiers as follows:

$$\left[(Q)(M_3)(P_3/P_0)(T_3/T_{AV})\right] \propto \left(\frac{W^4}{\rho_0 C_0 A^3 \rho_{AV}^2}\right)\left(\frac{2C_{p_{AV}} \Delta T\, g_c J}{V_{AV}^2}\right)\left(\frac{T_3^{3/2}}{T_{AV}\sqrt{T_0}}\right) \qquad (5)$$

With this rearrangement of terms, the combustion heat release rate and the flow terms can be expressed as an acoustic monopole source (term that includes W^4) modified by a temperature rise parameter and a temperature ratio.

Consideration of Combustor Geometry

In order to collapse the data shown in figure 5, on a single curve, the geometry of the combustors was introduced into the correlation. The primary variables considered were the number of burning sites (fuel nozzles), chamber size, burner staging, and fuel split between stages. With regard to chamber size, the important factors were the maximum area of the combustor and a characteristic burner length. The data correlation in the following sections is divided into three parts, the first two deal with single-stage coplanar burners while the third deals with multistage burners.

Single-Stage Coplanar Burners

The single-stage coplanar burners include all the configurations in which burning occurs in essentially one region of the combustion chamber. The two Vorbix configurations (JT3D-Vorbix and S-23 Vorbix) are also included in this category when the fuel split is 100/0 (i.e. burning with only the pilot stage operating).

Effect of number of fuel nozzles. - The acoustic data obtained with the JT8D-17 and J-52 combustors (ref. 6) were used to determine the effect of the number of fuel nozzles on the acoustic power level. These two combustion chambers were of the same size and shape and were operated over similar pressure, temperature, and air flow conditions. The J-52 combustor with its 4 fuel nozzles was of the order of 5 dB quieter than the JT8D-17 combustor at the same operating condition. This reduction in OAPWL was probably due to undetermined flame pattern and distribution changes within the combustor caused by the use of 4 nozzles rather than 1 nozzle, which may have resulted in a lowered stream tubulence level. In the absence of such measurements, the reduction in OAPWL is expressed in terms of the number of fuel nozzles used in each combustor. The data for the JT8D-17 and J-52 combustors were correlated, as shown in figure 6, by adding a factor $10 \log N_F^{0.775}$ to the OAPWL of equation (4), yielding the following proportionality:

$$OAPWL + 10 \log \left[1 + (P_3/P_D)^3\right] + 10 \log N_F^{0.775}$$

$$\propto 10 \log \left[QM_3(P_3/P_0)(T_3/T_{AV})\right] \quad (6)$$

Effect of chamber size. - In order to collapse the data shown in figures 5 and 6 to a single curve, the effect of combustor geometry was now considered. A geometry term given by the ratio of the maximum chamber cross-sectional area to the square of a characteristic chamber length achieved the desired data correlation. This term, A/ℓ_e^2, is entered in equation (6) as follows:

$$OAPWL + 10 \log \left[1 + (P_3/P_D)^3\right] + 10 \log N_F^{0.775} - 20 \log \left(A/\ell_e^2\right)$$

$$\propto 10 \log \left[QM_3(P_3/P_0)(T_3/T_{AV})\right] - 10 \log \left[1 + 0.67\left(A/\ell_e^2\right)^3\right] \quad (7)$$

where

$$\ell_e = \ell_1 \left[1 + 0.15(\ell_2/\ell_1)^5\right] \quad (8)$$

For combustors designed to operate only as single-stage burners, $\ell_e = \ell$. However, when a multistage combustor (JT8D-Vorbix, Vorbix S-23) is operated as a single-stage burner, as during an engine-idle condition, only the pilot nozzles are lit (100/0 fuel split). Under such an operating procedure, the flame may not be contained entirely within the length of the first stage burner. Consequently, a portion of the second stage burner length must be included in order to account for the excess flame size. For a two-stage burner, this leads to the concept of an effective characteristic chamber length, ℓ_e, where $\ell_e > \ell_1$ but $\ell_e < (\ell_1 + \ell_2)$. Because of the limited data available, extrapolation of ℓ_e to ratios of ℓ_2/ℓ_1 that exceed those of the combustors used herein should be treated with caution. The correlation of the data for single-stage burners and two-stage burners operating as single-stage burners is shown in figures 7

to 9. Note that in figure 7 the same single-burner data are shown as in figure 2. Excellent correlation of the data is achieved, with most data points within ±1 dB of the curve shown faired through the data. The few data points that deviate to significantly higher values than those obtained from the faired curve are associated with low flow rates and are believed to be contaminated by the cold flow noise floor. At the same time, the data in figure 8 that are significantly lower than the curve appear to have been over-corrected for cold flow effects in the applicable references.

Single-Stage Noncoplanar Burners

Single-stage noncoplanar combustors are those that have their pilot and main burners displaced axially in the same chamber. Examples of this type of combustor (see fig. 1(c)) are the Hybrid H-6 and Radial/Axial II-12 combustors in references 5 and 2, respectively. In order to correlate the data obtained with these configurations, the characteristic chamber length in the term $10 \log \left[1 + 0.67 \left(A/\ell_e^2\right)^3\right]$ is that measured from the downstream fuel nozzles to the combustor exit plane or $10 \log \left[1 + 0.67 \left(A/\ell_{min}^2\right)^3\right]$. The characteristic chamber length in the term $20 \log \left(A/\ell_e^2\right)$ remains the full length of the chamber measured from the upstream fuel nozzles to the combustor exit plane. The correlation of the H-6 and II-12 combustors is shown in figure 10. The deviation of some of the H-6 combustor data from the curve shown is attributed again to apparent excessive cold-flow corrections.

Multi-Stage Burner

With two-stage burning, such as used with the JT8D-Vorbix and the Vorbix S-23 (refs. 5 and 6, respectively), the effect of the fuel nozzles in each stage and the fuel split between the stages has to be included in a general correlation of the combustor noise data.

Effect of staged burning. - For the limited acoustic data available with two-stage burning, inclusion of a term consisting of a function of the ratio of the number of fuel nozzles in the second stage to those in the

first stage sufficed to correlate the data. This term is given by $10 \log \left[1 + 0.0625 \, (N_2/N_1)^4\right]$. This staging term must be included in the OAPWL term of equation (7).

Effect of fuel split. - The effect of fuel split with two-stage burners is relatively small, being of the order of 1 dB or less for the normal fuel splits used in the combustors tested. This effect, which also must be included in the OAPWL term of equation (5), can be expressed for the combustors tested by the following relationships:

$$\mathcal{F}(n) = 1.259 - 0.259 \sqrt{1 - \left(\frac{n - 100}{30}\right)^2} \qquad (9)$$

for $n \geq 70$ and

$$\mathcal{F}(n) = 1.259 - 0.259 \sqrt{1 - \left(\frac{n}{70}\right)^2} \qquad (10)$$

for $n < 70$.

The acoustic power correlation for two-stage burners is thus expressed as:

$$\begin{aligned} \text{OAPWL} + 10 \log \left[1 + (P_3/P_D)^3\right] + 7.75 \log N_F - 20 \log \left(A/\ell_c^2\right) \\ - 10 \log \left[1 + 0.0625 \, (N_2/N_1)^4\right] + 10 \log \mathcal{F}(n) \\ = 10 \log \left[QM_3(P_3/P_0)(T_3/T_{AV})\right] - 10 \log \left[1 + 0.67 \left(A/\ell_c^2\right)^3\right] \end{aligned} \qquad (11)$$

The data for the JT8D-Vorbix and the Vorbix S-23 are shown correlated in figure 11 in terms of equation (11). The curve shown in figure 11 is the same as that shown previously in figures 7 to 10 for the single stage burners. In general, good correlation of the data is obtained with only a few data points significantly off of the correlation curve. Again, it appears that some of the S-23 data are over-corrected for cold-flow effects.

Correlation Equation

The curve shown faired through the data in figures 7 to 11 can be expressed by:

$$OAPLW^* = 5 \log(Q^* Q_{REF}) + \frac{69.0}{\left(1 + \frac{0.33 \times Q^*_{REF}}{Q^*}\right)} - 85.0 \qquad (12)$$

where $Q^*_{REF} = 10^{17}$ and, from equation (11),

$$OAPWL^* = OAPWL + 10 \log\left[1 + (P_3/P_D)^3\right] + 7.75 \log N_F - 20 \log A_e^2$$

$$- 10 \log\left[1 + 0.0625 (N_2 - N_1)^4\right] + 10 \log S_F(n)$$

and

$$Q^* = \left[QM_3 (P_3/P_0)(T_3/T_{AV})\right]^3 \left[1 + 0.67 A_e^2\right]^3$$

A summary of all the data included in figures 7 to 11 is shown in figure 12 in terms of the final correlation parameters (eq. (11)) together with the correlation curve (eq. (12)).

CONCLUDING REMARKS

A correlation of published acoustic power levels, inferred from fluctuating pressure measurements, has been developed. The correlation includes acoustic data obtained with can-type, annular and reverse-flow annular combustors over a wide range of operating conditions. The correlation further includes acoustic data obtained with both combustion development component rigs and engines.

With the present correlation, the OAPWL can be predicted for a specific combustor. The sound pressure levels and frequency content can then be calculated by use of a suitable combustion noise spectral shape

(such as given in refs. 11 and 12) together with OAPWL values from the present correlation. With this information, the combustion noise in the far-field can be calculated by considering the applicable turbine, nozzle and atmospheric transmission losses.

On the basis of the parameters included in the correlation presented herein (eq. (12)) the following, assuming independence, will cause a reduction in combustor overall power levels:

1. Increase in total number of fuel nozzles (burning sites)
2. Staged burning with large ratios of N_2/N_1 (i.e. greater number of fuel nozzles in second stage than in primary stage)
3. Increase in combustor area, A
4. Decrease in combustor length, ℓ_c
5. Decrease in combustor inlet, P_3
6. Decrease in combustion heating rate, Q
7. Decrease in combustor inlet Mach number, M_3
8. Decrease in combustor inlet temperature ratio, T_3/T_{AV}

In order to achieve a meaningful reduction in combustor power level, it does not appear that significant design or operating changes in the preceding variables can be made without incurring other and, in most cases, prohibitive penalties. On the basis of the currently available data, it appears that substantial combustor noise reductions can be make in a practical manner only by resorting to suitable tailpipe lining techniques.

NOMENCLATURE

(All symbols are in S.I. units unless noted.)

A	maximum combustion chamber cross-sectional area
C	velocity of sound
C_p	specific heat of air
F_b	fuel/air ratio
F_{ST}	stoichiometric fuel/air ratio
$\mathcal{F}( )$	functional notation
g_c	conversion constant

H_F	heating value of fuel
J	mechanical equivalent of heat
ℓ	combustion chamber total length
ℓ_e	equivalent combustion chamber length
$\ell_1, \ell_2, \ldots, \ell_n$	physical length of each combustor burner stage
M	Mach number at combustor inlet
N_F	total number of fuel nozzles
$N_1, N_2, \ldots, N_n$	number of active fuel nozzles in each burner stage
n	burner stage fuel split (see eqs. (9) and (10))
OAPWL	overall sound power level, dB re 10^{-13} watts
OAPWL*	acoustic power correlation parameter (see eq. (12))
P	combustion chamber total pressure
Q	combustion heat release rate
Q*	combustion heat release rate parameter (see eq. (12))
T	total temperature
ΔT	temperature rise due to combustion
V	combustion airflow velocity
W	total combustion airflow rate
η	thermoacoustic efficiency, OAPWL = 10 log Q
ρ	density

Subscripts:

AV	average
D	design
0	atmospheric
REF	reference
3	nominal combustion chamber inlet
4	nominal combustion chamber outlet

REFERENCES

1. H. Kozlowski, A. Packman, and O. Gutierrez, "Aeroacoustic Performance Characteristics of Duct Burning Turbofan Exhaust Nozzles," AIAA Paper 76-148 (January 1976).

2. J. J. Emmerling, "Experimental Clean Combustor Program, Phase I, Noise Measurement Addendum," NASA CR-134853 (July 1975)

3. J. J. Emmerling, and K. L. Bekofske, "Experimental Clean Combustor Program, Phase II, Noise Measurement Addendum," NASA CR-135045 (January 1976).

4. T. G. Sofrin, and D. A. Ross, "Experimental Clean Combustor Program, Phase I, Noise Addendum," NASA CR-134820 (October 1975).

5. T. G. Sofrin, and N. Rikoff, Jr., "Experimental Clean Combustor Program--Noise Study," NASA CR-135106 (September 1976).

6. D. Mathews, N. Rekos, Jr., and R. Nagel, " Combustion Noise Investigation," PWA-5478 (FAA RD-77-3), Pratt and Whitney Aircraft Group, United Technologies Corporation (February 1977).

7. E. A. Burdsall, F. P. Brochu, and V. M. Scaramella, "Results of Acoustic Testing of the JT8D-109 Refan Engines," NASA CR-134875 (November 1975).

8. M. Reshotko, A. Karchmer, P. F. Penko, and J. G. McArdle, "Core Noise Measurements on a YF-102 Turbofan Engine," NASA TM X-73587 (January 1977).

9. R. K. Matta, G. T. Sandusky, and V. L. Doyle, "G.E. Core Engine Noise Investigations - Low Emission Engines," General Electric Co. FAA RD-77-4 (February 1977).

10. S. H. Guest, "Acoustic Efficiency Trends for High Thrust Boosters," NASA TN D-1999 (July 1964).

11. R. Motsinger, "Prediction of Engine Combustor Noise and Correlation with T-64 Engine Low Frequency Noise," R72AEG313, General Electric Co. (1972).

12. R. G. Huff, B. J. Clark, and R. G. Dorsch, "Interim Prediction Method for Low Frequency Core Engine Noise," NASA TM X-71627 (November 1974).

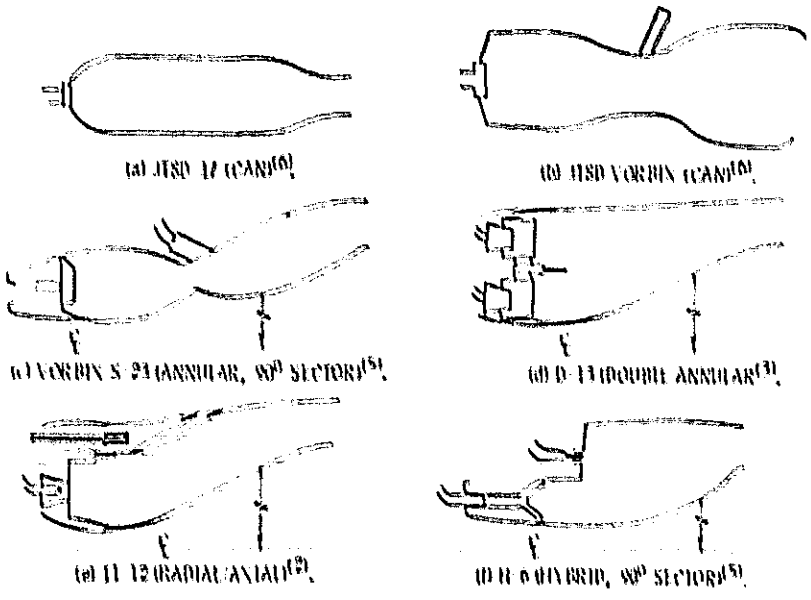

Figure 1. – Schematic sketches of representative combustors. (Not to scale.)

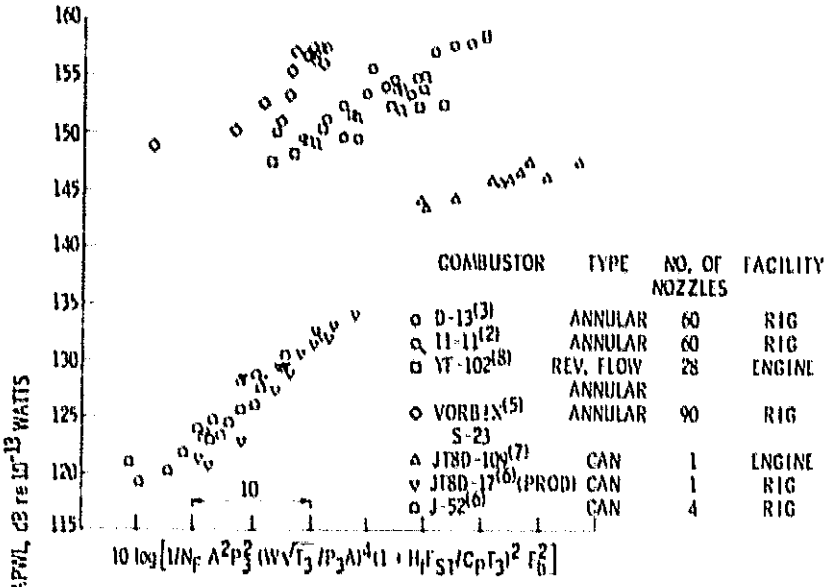

(a) PRATT AND WHITNEY AIRCRAFT CORRELATION, REF. 6.

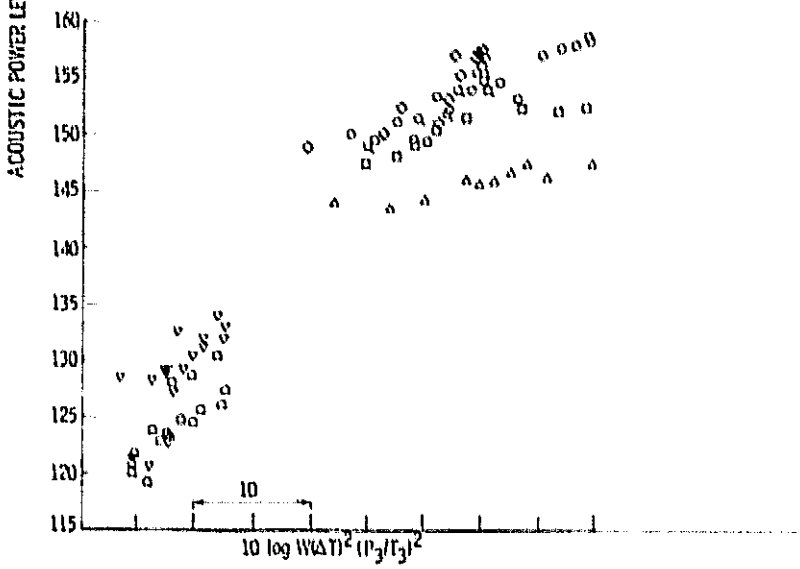

(b) GENERAL ELECTRIC CORRELATION; ENGINE PARAMETERS, REF. 9.

Figure 2. - Current combustion noise correlations applied to representative combustor data.

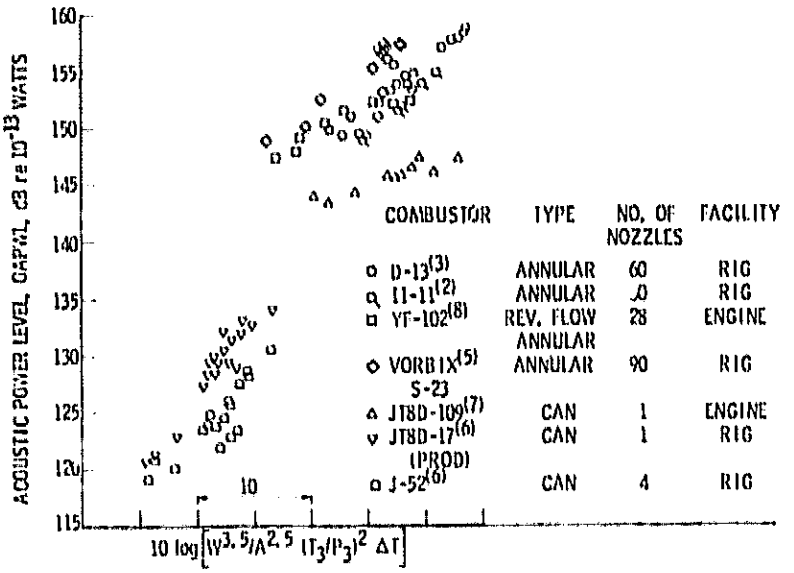

(c) GENERAL ELECTRIC CORRELATION; RIG PARAMETERS, REF. 9.

Figure 2. - Concluded.

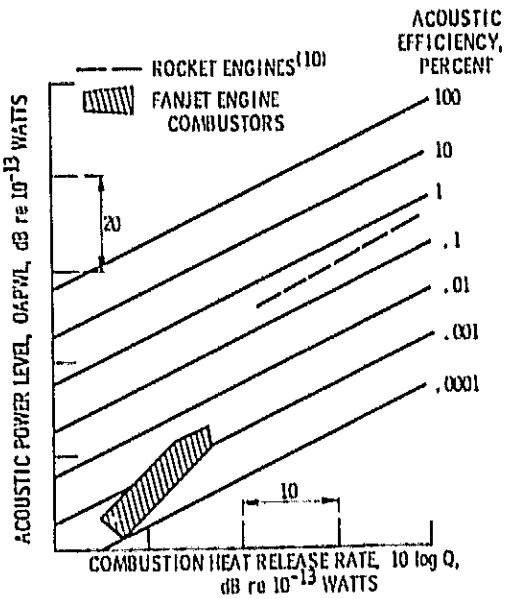

Figure 3. - Thermo-acoustic efficiency of fanjet and rocket engine combustion chambers.

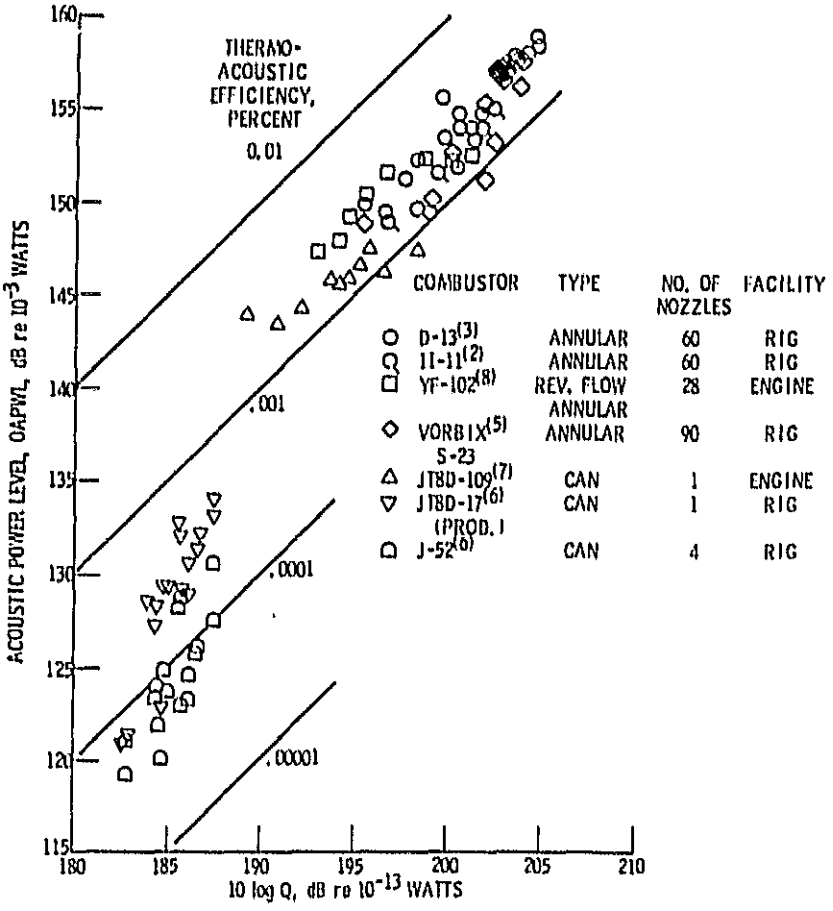

Figure 4. - Variation of acoustic power level with combustion heat release rate for representative combustors.

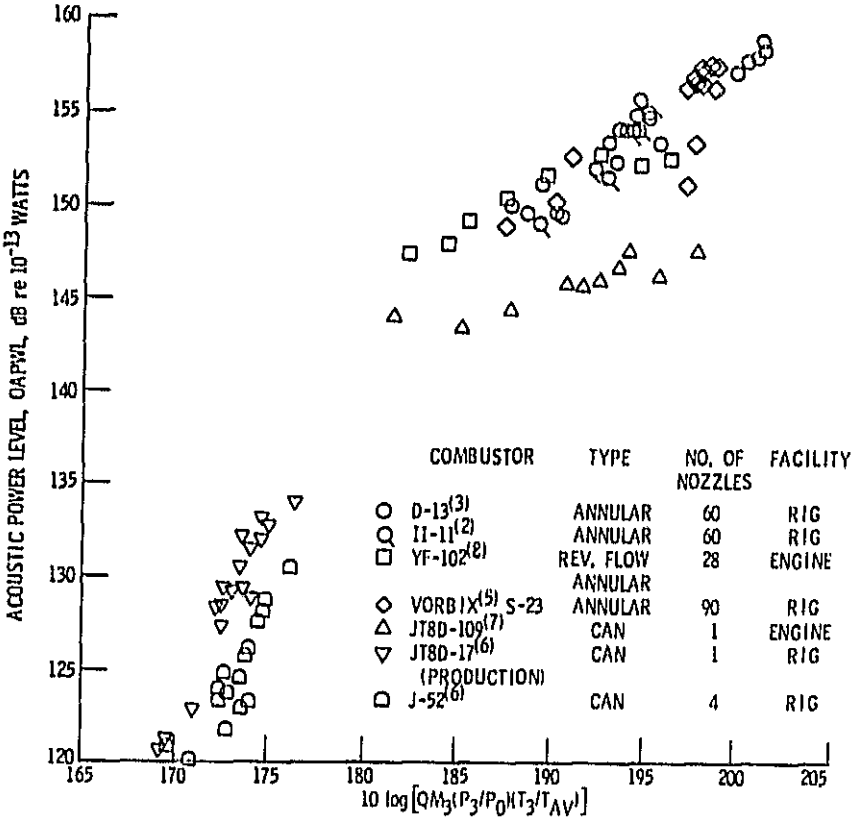

Figure 5. - Variation of OAPWL with combustion heat release rate and flow parameters.

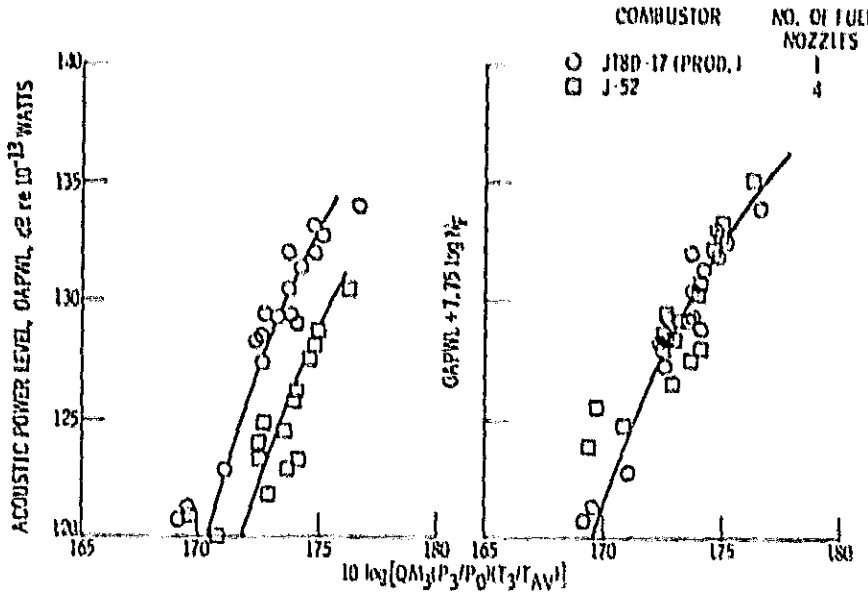

Figure 6. - Variation of combustor acoustic power level with number of fuel nozzles. Nominal airflow, 0.53 - 0.70 kg/sec; nominal pressure ratio, 1.12 atm; reference 6.

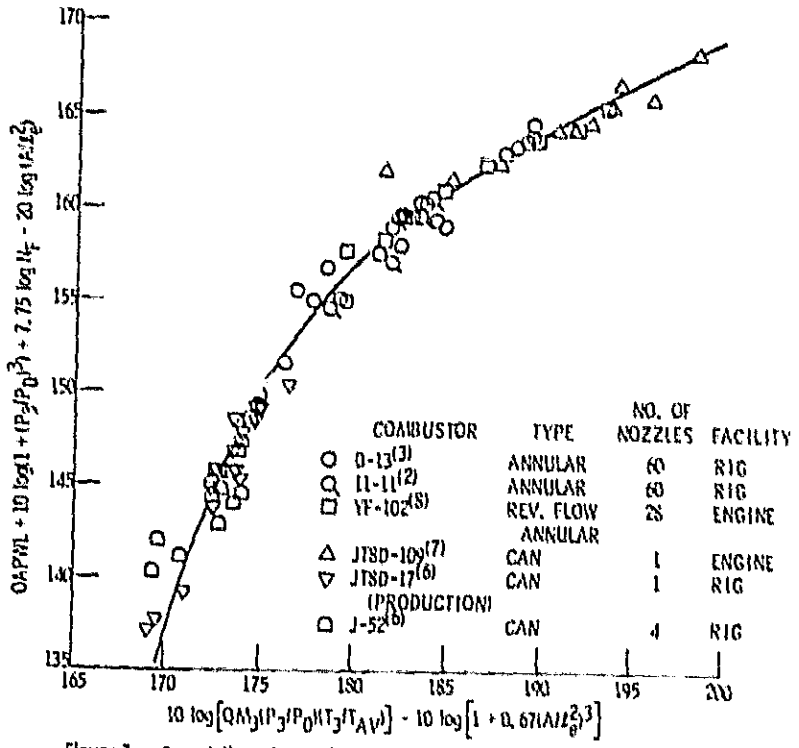

Figure 7. - Correlation of acoustic power levels for selected single-stage combustors.

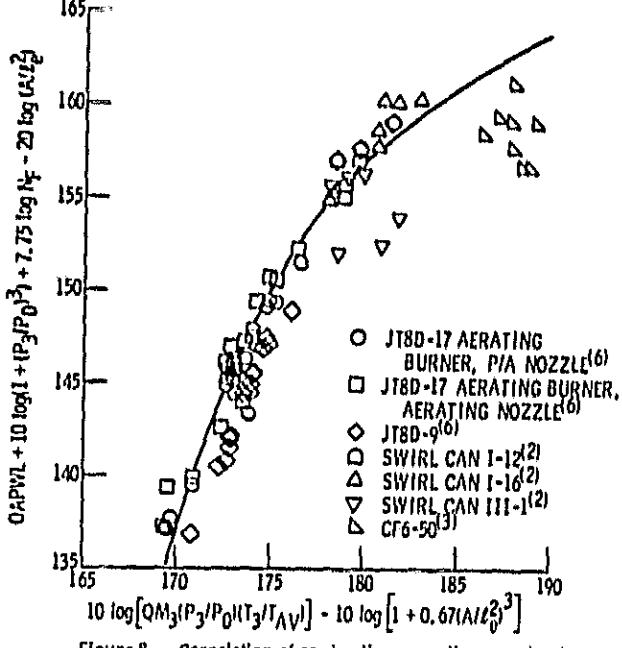

Figure 8. - Correlation of combustion acoustic power levels for miscellaneous can and annular combustors. Single-stage burners.

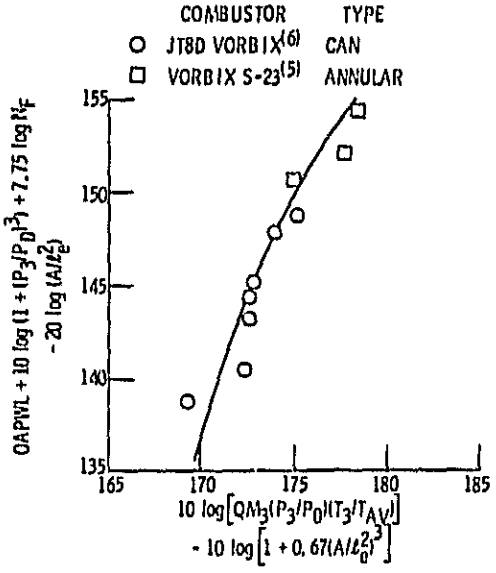

Figure 9. - Correlation of combustion acoustic power levels for 2-stage burners with burning in the first stage only.

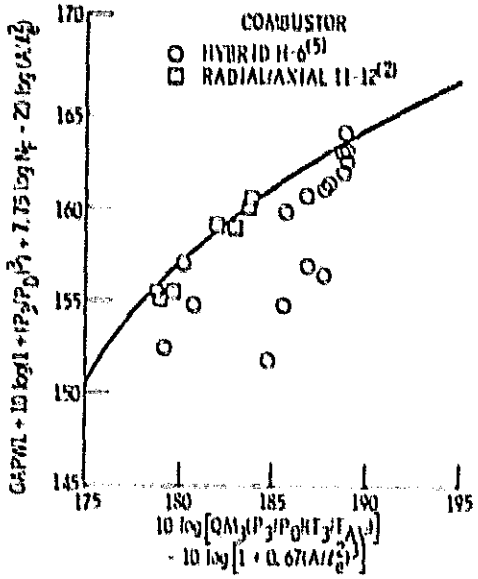

Figure 10. - Correlation of acoustic power levels for noncoplanar nozzle arrays in single-stage combustors.

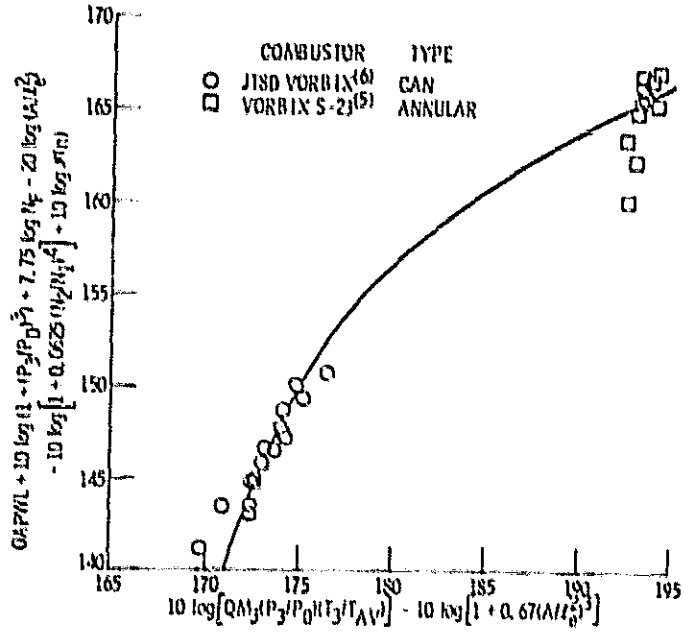

Figure 11. - Correlation of acoustic power levels for 2-stage burner combustors.

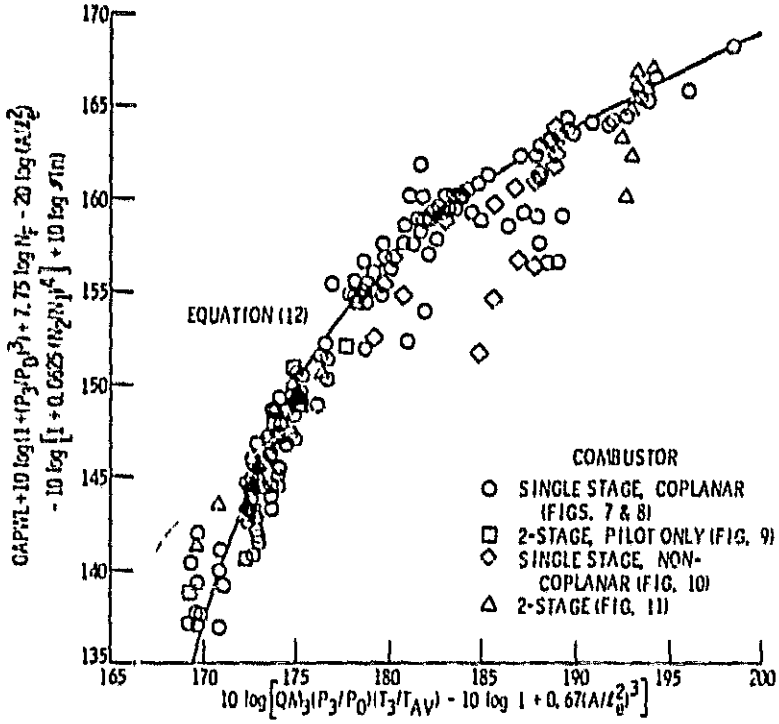

Figure 12. - Summary of data correlation for all combustors included in present study.

1. Report No.	2. Government Accession No.	3. Recipient's Catalog No.
NASA TM-78988		

4. Title and Subtitle	5. Report Date
CORRELATION OF COMBUSTOR ACOUSTIC POWER LEVELS INFERRED FROM INTERNAL FLUCTUATING PRESSURE MEASUREMENTS	6. Performing Organization Code

7. Author(s)	8. Performing Organization Report No.
U. H. von Glahn	E-0764
	10. Work Unit No.

9. Performing Organization Name and Address	11. Contract or Grant No.
National Aeronautics and Space Administration Lewis Research Center Cleveland, Ohio 44135	

12. Sponsoring Agency Name and Address	13. Type of Report and Period Covered
National Aeronautics and Space Administration Washington, D.C. 20546	Technical Memorandum
	14. Sponsoring Agency Code

15. Supplementary Notes

16. Abstract

Combustion chamber acoustic power levels inferred from internal fluctuating pressure measurements are correlated with operating conditions and chamber geometries over a wide range. The variables include considerations of chamber design (can, annular, and reverse-flow annular) and size, number of fuel nozzles, burner staging and fuel split, airflow and heat release rates, and chamber inlet pressure and temperature levels. The correlated data include those obtained with combustion component development rigs as well as engines.

17. Key Words (Suggested by Author(s))	18. Distribution Statement
Combustor noise	Unclassified - unlimited STAR Category 71

19. Security Classif. (of this report)	20. Security Classif. (of this page)	21. No. of Pages	22. Price*
Unclassified	Unclassified		

* For sale by the National Technical Information Service, Springfield, Virginia 22161